BBA - Biomembranes 1860 (2018) 2588–2598

Contents lists available at ScienceDirect

BBA - Biomembranes

journal homepage: www.elsevier.com/locate/bbamem

Casein interaction with lipid membranes: Are the phase state or charge density of the phospholipids affecting protein adsorption?

Adrián Crespo-Villanueva[a,b,c,e,1], Berta Gumí-Audenis[a,b,c,1], Fausto Sanz[a,b,c], Franck Artzner[d], Cristelle Mériadec[d], Florence Rousseau[e], Christelle Lopez[e], Marina I. Giannotti[a,b,c], Fanny Guyomarc'h[e,*]

[a] Institute for Bioengineering of Catalonia (IBEC), Barcelona Institute of Science and Technology (BIST), Barcelona, Spain
[b] Material Sciences and Physical Chemistry Department, Universitat de Barcelona, Barcelona, Spain
[c] Centro de Investigación Biomédica en Red (CIBER), Instituto de Salud Carlos III, Madrid, Spain
[d] Institut de Physique de Rennes, UMR 6251, CNRS, Université de Rennes 1, Rennes, France
[e] Science and Technology of Milk and Egg (STLO), INRA, Agrocampus Ouest, 35000 Rennes, France

ARTICLE INFO

Keywords:
Casein proteins
Phospholipid membrane
Supported lipid bilayer
Atomic force microscopy

ABSTRACT

Casein micelles are ~200 nm electronegative particles that constitute 80 wt% of the milk proteins. During synthesis in the lactating mammary cells, caseins are thought to interact in the form of ~20 nm assemblies, directly with the biological membranes of the endoplasmic reticulum and/or the Golgi apparatus. However, conditions that drive this interaction are not yet known. Atomic force microscopy imaging and force spectroscopy were used to directly observe the adsorption of casein particles on supported phospholipid bilayers with controlled compositions to vary their phase state and surface charge density, as verified by X-ray diffraction and zetametry. At pH 6.7, the casein particles adsorbed onto bilayer phases with zwitterionic and liquid-disordered phospholipid molecules, but not on phases with anionic or ordered phospholipids. Furthermore, the presence of adsorbed caseins altered the stability of the yet exposed bilayer. Considering their respective compositions and symmetry/asymmetry, these results cast light on the possible interactions of casein assemblies with the organelles' membranes of the lactating mammary cells.

1. Introduction

Caseins are a family of natively unfolded and phosphorylated proteins that constitute a distinctive fraction of the milk proteins. The β-casein, κ-casein, α_{s1}- and α_{s2}-caseins are 19–25 kDa and represent the four major and well-characterized casein species of bovine milk [1]. Their isoelectric point (pI) is 4.9–5.8 depending on the variant and, unlike other natively unfolded proteins, they bear significant hydrophobicity [2]. Caseins therefore readily associate in aqueous medium, as early as during protein synthesis in the rough endoplasmic reticulum (ER) of the lactating mammary cells [3]. Hydrophobic-mediated casein association is thought to promote transport toward the Golgi apparatus, where caseins form particles of ~20 nm diameter, sometimes bound to the Golgi membranes [4]. At a late stage, phosphorylation of the caseins triggers supra-aggregation into ~200 nm casein micelles through calcium and calcium phosphate bridging, prior to their release into the milk secretion [3,4]. During this process, it has been hypothesized that α_{s1}-casein acted as an “escort” protein during ER-to-Golgi transport of the early casein aggregates, through its propensity to bind both the other caseins and the membrane of ER microsomes [5]. The association of κ-casein with either α_{s1}- or β-caseins was also reported to increase the affinity of κ-casein for phospholipid membranes, and to prevent extended amyloid fibrillation of κ-casein that otherwise occurs when interacting alone with membranes [6]. Therefore, the interaction of the early casein aggregates with biological membranes is an important issue to casein trafficking within the lactating cell, and to the control of self-association of the four caseins into casein particles rather than pathogenic fibrils.

Long-range attraction between protein and phospholipid membranes in aqueous media is essentially driven by electrostatic interaction [7,8]. At close distance, ion-pair, hydrophobic effects and van der Waals interactions ensure stable binding of peripheral proteins and, to some extent, the penetration of the protein's hydrophobic, tryptophan-rich regions into the phospholipid bilayer [7,9–11]. Discrete or local

* Corresponding author.
E-mail address: fanny.guyomarc-h@inra.fr (F. Guyomarc'h).
[1] These authors contributed equally.

https://doi.org/10.1016/j.bbamem.2018.09.016
Received 9 July 2018; Received in revised form 11 September 2018; Accepted 26 September 2018
Available online 28 September 2018

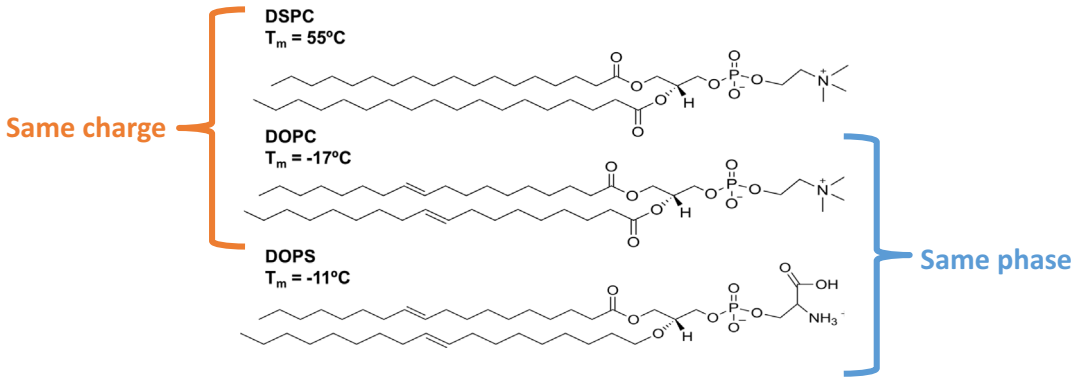

Fig. 1. Molecular structures and indicative melting temperatures (T_m) of 1,2-distearoyl-*sn*-glycero-3-phosphocholine (DSPC), 1,2-dioleoyl-*sn*-glycero-3-phosphocholine (DOPC) and 1,2-dioleoyl-*sn*-glycero-3-phosphoserine (DOPS - Avanti Polar Lipids).

variations in the protein's structure also affect binding at molecular level [7,12]. Polarization (or dipole) effect may drive efficient adsorption of, e.g., an overall negatively charged protein with positive patches, onto a negatively-charged bilayer, and 4–5 ion pairs may be enough to achieve irreversible binding [7,13]. The presence of phosphate groups or calcium counter-ions, which are both relevant for caseins, can also affect local electrostatic interactions [7]. Finally, bound and organized water molecules at the surface of bilayers with low polarizability and an environment of low dielectric constant repulse proteins from the interface [8,14]. Hence, desolvation inhibits protein-membrane binding, but this effect is modulated by protonation of protein's ionized groups, which itself can depend on the local environment exerted by the ionic nature of the phospholipids [7,15]. Finally, the phase state of the phospholipid bilayer is susceptible to affect protein adsorption and function [16,17]. Therefore, the goal of this study was to evaluate the role of phase and charge of the phospholipid membrane onto its interaction with caseins.

Different methods are available to investigate protein interaction with membranes, among which dissipative quartz crystal microbalance, surface plasmon resonance, isothermal titration calorimetry, neutron or X-ray reflectivity, Fourier-transform infrared reflection-absorption spectroscopy or nuclear magnetic resonance [9,18–21]. Change in the environment of fluorescent probes is also used to monitor protein adsorption onto liposomes [6,17,22]. However, these methods average information from large numbers of individual behaviors. In contrast, high-resolution microscopy such as atomic force microscopy (AFM) allows observations of protein-membrane interactions at the nanoscale, relevant for potentially multiphasic membranes [16,23–26]. To date, the only AFM observations of casein-membrane interaction were on Langmuir films where β-casein was compressed together with the polar lipid monolayer, then dehydrated [27–29]. This approach was relevant to investigate the behavior of β-casein and phospholipids as emulsifiers, but not to describe the factors that drive interaction of casein particles with biological membranes. In the present study, AFM imaging was used to directly observe the interaction of caseins with model phospholipid bilayers presenting distinct phase or charge states, in aqueous environment at 20 °C and at pH 6.7. Sodium caseinate, rather than isolated caseins, was used as means to model the early ~20 nm casein particles present in the ER, which are thought to interact with organelle membranes during the ER-to-Golgi transport, prior to the casein micelle final assembly.

2. Experimental methods

2.1. Materials

Caseinates are prepared from the milk's casein micelles through elimination of the calcium-mediated bridges in order to part the assembly into ~20 nm particles (e.g. [30–32]). The sodium caseinate used in this study was manufactured by Armor Protéines (Saint Brice en Coglès, France). It was prepared through acid-precipitation of milk, exhaustion of calcium phosphate through washing then alkalization with sodium hydroxide. It contained > 94 wt% casein over dry matter, < 3.9 wt% ashes and 0.8 wt% non-casein nitrogen (peptides, urea… [33]). Sodium caseinate was dispersed at 1 mg·mL^{-1} in PIPES (1,4-piperazinediethanesulfonic acid) buffer at ~40 °C, then stored overnight at 5 °C to ensure complete dispersion and used on the following day.

PIPES buffer was prepared using PIPES 10 mM (purity ≥ 99 wt%; Sigma-Aldrich, Milwaukee, WI, USA), NaCl 50 mM (purity ≥ 99 wt%; Sigma-Aldrich), and $CaCl_2$ 0.1 mM (purity ≥ 99 wt%; Sigma-Aldrich) dissolved in ultrapure Milli-Q water and adjusted to pH 6.7 using NaOH 5 M. The ionic strength μ of the buffer was calculated to be $\mu = 0.05025$ mol·L^{-1}.

Synthetic 1,2-distearoyl-*sn*-glycero-3-phosphocholine (C18:0 DSPC; purity > 99 wt%), 1,2-dioleoyl-*sn*-glycero-3-phosphocholine (C18:1 DOPC; purity > 99 wt%) and 1,2-dioleoyl-*sn*-glycero-3-phosphoserine (C18:1 DOPS; purity > 99 wt%) were purchased from Avanti Polar Lipids (Alabaster, AL, USA). All three phospholipids are 18 carbons in length; DSPC is saturated while DOPS and DOPC exhibit one unsaturation (Fig. 1).

Therefore, the molecules differ either in their melting temperatures, hence in their phase state at 20 °C: both DOPC and DOPS are expected to be in liquid-disordered (l_d) phase at 20 °C while DSPC is expected to be in the solid-ordered (s_o) phase at that temperature. Meanwhile, DOPS bears an anionic polar head while DOPC and DSPC's head is zwitterionic.

2.2. Sample preparation

Multilamellar vesicles (MLVs) of the pure DOPC, DSPC or DOPS were required for physical characterization. Small unilamellar vesicles (SUVs) were required for zeta potential measurement or for preparation of supported lipid bilayers (SLBs). SLBs were manufactured with two co-existing phases, differing either in phase state or in charge. Namely, DOPC/DSPC 50/50 mol% bilayers were expected to exhibit domains DSPC-rich in the s_o phase, dispersed in the continuous DOPC-rich l_d phase. Meanwhile, 0.1 mM calcium in the environment was expected to induce separation in DOPC/DOPS 50/50 mol% bilayers in distinct enriched phases differing in local charge, as reported for s_o-s_o phase separation in 1,2-dipalmitoyl-*sn*-glycero-3-phosphocholine/1,2-dipalmitoyl-*sn*-glycero-3-phosphoserine (DPPC/DPPS) bilayers [34].

First, accurate mother solutions of each lipid were prepared in chloroform/methanol (4:1 v/v) into glass vials. Dried lipid films were then prepared by mixing the appropriate volumes of the mother solutions into glass vials, followed by evaporation of the solvent at 40 °C

under a gentle stream of dry nitrogen, then storage at −20 °C. After equilibration at room temperature, the dried lipid films were hydrated with PIPES buffer at 70 °C to reach a final concentration of 0.1 wt%, then thoroughly vortexed to yield microscopic multilamellar vesicles (MLVs). Then, small unilamellar vesicles (SUVs) were produced by sonication at 70 °C using a Q700 equipment (Q-sonica, Newtown, CT, USA) and a microtip operating at 50% amplitude (~400 W) for 1 h.

2.3. Differential scanning calorimetry

The thermotropic properties of DSPC, DOPC or DOPS were measured on MLVs using a differential scanning calorimetry (DSC) Q1000 apparatus (TA Instruments, New Castle, DE, USA). MLVs were produced by rehydration of the lipid films with PIPES buffer at 70 °C to reach a final concentration of 20 wt% lipids, then thoroughly vortexed and left to equilibrate at room temperature. MLVs accommodate high bilayer concentration; they also allow increased resolution thanks to cooperativity of the molecules [35]. The samples were introduced in 20 μL aluminum pans that were then hermetically sealed. An empty pan was used as a reference. The samples were heated at 2 °C·min^{-1} from −40 °C to 70 °C. The calibration of the calorimeter was performed with indium standard (melting point = 156.66 °C, ΔH melting = 28.41 J·g^{-1}). The thermal measurements were performed in triplicate. Standard parameters were calculated by the TA software (Universal Analysis 2000, v 4.1 D).

2.4. X-ray diffraction

X-ray diffraction (XRD) experiments were performed on the same MLVs suspensions of DSPC, DOPC or DOPS as in DSC, using the home-made Guinier beamline at IPR [36]. A two-dimensional Pilatus detector with sample to detector distance of 232 mm allowed the recording of XRD patterns in the range 0.013 Å^{-1} to 1.742 Å^{-1}, thus covering both the small and wide-angles regions of interest to characterize the lamellar structures and to identify the packing of the acyl chains, respectively. Diffraction patterns displayed series of concentric rings as a function of the radial scattering vector $q = 4\pi\sin\theta/\lambda$, where 2θ is the scattering angle and λ = 1.541 Å is the wavelength of the incident beam. The channel to scattering vector q calibration of the detector was carried out with silver behenate [37]. The vesicle suspensions (~10 μL at 20 wt%) were loaded in thin quartz capillaries of 1.5 mm diameter (GLAS W. Muller, Berlin, Germany) and analyzed at 20 or 70 °C.

2.5. Dynamic light scattering

The hydrodynamic diameter Dh of the SUVs and of the sodium caseinate suspension was measured by dynamic light scattering (DLS) at 20 °C and in PIPES buffer using a Zetasizer Nano ZS (Malvern Instruments, Worcestershire, UK) operating at a scattering angle of 173° and a wavelength of 633 nm. The mean Dh was calculated from the intensity distribution using the Stokes-Einstein relation assuming spherical objects. Viscosity of the buffer was taken as 1.003 mPa·s at 20 °C. The refractive index of the buffer was taken as 1.33. Measurements were performed in triplicate. The mean Dh of DSPC/DOPC 50/50 mol% or DOPC/DOPS 50/50 mol% SUVs was of 164 or 139 nm (± 5 nm), respectively, with a polydispersity index of 0.2.

2.6. Zetametry

The zeta potential ζ of DOPC, DSPC, DOPS or DOPC/DOPS 50/50 wt % SUVs, as well as that of the sodium caseinate particles were measured in PIPES buffer at 20 °C and at pH 6.7 using the same Zetasizer Nano ZS equipment as for DLS. The electrophoretic mobility μ_e, in $m^2.V^{-1}.s^{-1}$, was measured at 50 V. The viscosity η and dielectric constant ε_r of the buffer were taken as 1.003 mPa.s and 78.5, respectively. ζ was calculated from μ_e using the Smoluchowski relationship:

$\mu_e = \varepsilon_r\varepsilon_0\zeta/\eta$ where ε_0 is the dielectric constant of vacuum. This relationship is valid as the Debye length, calculated to be 1.36 nm in PIPES buffer, was negligible with respect to the radius of the particles. From this, the surface charge density σ, in C·m^{-2}, of the bilayers was calculated using the Grahame relationship:

$\sigma = \varepsilon_r\varepsilon_0 k\zeta$ with k the reciprocal of the Debye length [38]. Measurements were performed in triplicate.

2.7. Atomic force microscopy

Formation of planar SLBs of either DSPC/DOPC 50/50 mol% or DOPC/DOPS 50/50 mol% phospholipid mixtures was performed using vesicle fusion [39]. To do this, 2.7 mL of PIPES buffer were pre-heated at 70 °C using open liquid cells (Asylum Research, Oxford Instruments, Santa Barbara, CA, USA) mounted with freshly cleaved mica. Then, 300 μL of the hot SUV suspension were injected into the liquid cell, to reach 0.01 wt% lipids. The samples were incubated at 70 °C for 1 h using an IPP programmed incubator (Memmert, Büchenbach, Germany) and saturated humidity chambers to prevent evaporation, then slowly cooled down to 20 °C with rates sequentially decreasing from ~1 °C·min^{-1} to ~0.1 °C·min^{-1} in 3 h. The bilayers were then extensively and gently rinsed with PIPES buffer. Atomic force microscopy (AFM) imaging was performed in contact or AC mode using two MFP-3D Bio AFM (Asylum Research, Santa Barbara, CA, USA) at IBEC or STLO. Silicon MSNL probes (Bruker AFM Probes, Camarillo, CA, USA) were used for contact mode imaging (nominal spring constant k ~0.03 N·m^{-1}) while silicon nitride SNL probes (Bruker AFM Probes, Camarillo, CA, USA) were used for AC mode imaging (nominal spring constant k ~ 0.35 N·m^{-1} for DSPC/DOPC bilayers or ~0.12 N·m^{-1} for DOPC/DOPS bilayers) calibrated extemporaneously using the thermal noise method. Imaging loading forces were typically below ~1 nN. The typical scan speed was 15 μm·s^{-1} for 5 × 5 μm^2 (256 × 256 pixels) images. Images were 3:30 or 4 min to take and were recorded continuously prior to and after injection of 50 μg of sodium caseinate in the 3 mL volume of the liquid cell. No stirring was possible, precluding precise information on the delay until adsorption. Scanning angle was 90° in order to calculate friction from calculation of the trace minus retrace error signals. Final temperature inside the liquid cell was 22.3 ± 0.8 °C, due to heating by e.g. the AFM laser. The images were typically planefitted at order 0, flattened at order 1 and then planefitted again after masking of the protruding domains. Sections were drawn across images to measure the height difference H between features of the images.

In AFM-based force spectroscopy (AFM-FS) experiments, force-distance curves were recorded after imaging an interesting area, by approaching and retracting the cantilever tip to the sample at constant velocity of 1 μm·s^{-1}. SNL probes were used, with nominal spring constants of 0.35 N·m^{-1} and 0.12 N·m^{-1}, setting maximal forces of 65 nN and 15 nN, respectively. The cantilever spring constants were individually calibrated by using the equipartition theorem (thermal noise routine). Force-separation curves were acquired in the force map mode, using an array of 20 × 20 pixels.

3. Results & discussion

3.1. Physicochemical properties of sodium caseinate

Sodium caseinate particles in suspension ranged from 5 to 50 nm in diameter and exhibited an average hydrodynamic diameter Dh of 19 ± 1 nm (Fig. 2), in agreement with previous reports [30–32]. Their zeta potential ζ in PIPES buffer at pH 6.7 and at 20 °C was −12.7 ± 0.6 mV, corresponding to a surface charge density of −0.0066 C·m^{-2}.

Considering their pI, individual caseins and their assemblies are expected to bear negative charge at pH 6.7, but amplitude depends on the temperature and presence of counter-ions [40,41]. In pure water or

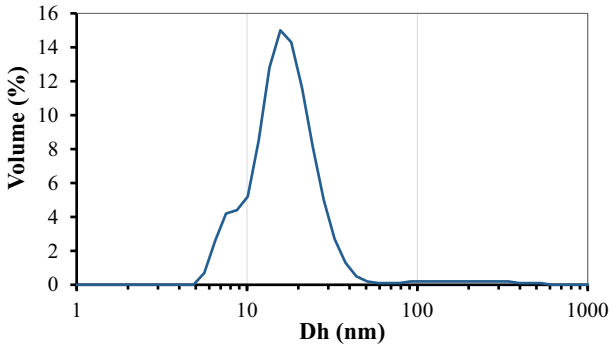

Fig. 2. Average dynamic light scattering distribution in volume of the hydrodynamic diameter Dh of 1 mg·mL^{-1} sodium caseinate in PIPES/NaCl/0.1 mM $CaCl_2$ buffer at pH 6.7 and at 20 °C.

in 10 mM NaCl, commercial sodium caseinate exhibits a value ζ of −42 mV [42] or −25 mV [43], respectively. The presence of 50 mM NaCl and 0.1 mM $CaCl_2$ in the PIPES buffer probably accounts for the lower absolute ζ value determined in the present conditions.

3.2. Physicochemical properties of phospholipids assembled into hydrated bilayers

The melting temperatures T_m recorded with DSC for fully hydrated DSPC, DOPC and DOPS vesicles in PIPES buffer were +54.2, −19.8 and −11.8 °C, respectively (Fig. 3A), in agreement with previous reports [44–46]. For identical acyl chain lengths, unsaturation is well known to decrease T_m. Furthermore, PS head-group yields closer packing of the phospholipids in the bilayers and higher T_m value than for their respective PC counterparts [45,47].

At small angle, X-ray scattering spectra showed Bragg diffraction peaks for DSPC and DOPC due to the multilamellar organization of the neutral phospholipids (Fig. 3B). Repeat spacing was 6.6–6.7 nm in both types of bilayers; previous reports range 6.3–7 nm e.g. for DOPC or DSPC, depending on conditions [47–49]. Upon heating to 70 °C, the reciprocal distance between DSPC peaks slightly increased, indicating thinner bilayers upon melting (Fig. 3B, q < 0.5 Å^{-1}). At wide angle, XRD spectra are informative on the lateral packing of the phospholipid molecules. Expectedly, DOPC exhibited no sign of lateral order neither at 20 °C nor at 70 °C, indicating disordered liquid-crystalline (L_α or l_d) phase (Fig. 3B). DSPC exhibited a clear single peak at q = 1.465 Å^{-1} and a diffuse scattering at q = 1.552 Å^{-1} at 20 °C. This is characteristic of a s_o hexagonal packing of the acyl chains with an important tilt toward the next neighbor [50,51]. The intermolecular distance was ~4.3 Å, slightly lower than that previously reported in water [49]. For anionic DOPS, a diffusion peak at small angle overlapped with the diffraction signature, possibly indicating more frequent unilamellar vesicles and/or less bilayer stacking due to electrostatic repulsion between the PS head-groups [47]. As for DOPC, DOPS at wide angle exhibited no sign of lateral order neither at 20 °C nor at 70 °C (Fig. 3B). In brief, DSC and XRD experiments clearly confirmed that DOPC and DOPS were in liquid-disordered (l_d or L_α) phase at 20 °C, while DSPC assumed a solid-ordered (s_o or L_β) phase at the working temperature, in agreement with the respective unsaturation/saturation of their acyl chains.

The surface charge density, σ, of small unilamellar vesicles of DSPC

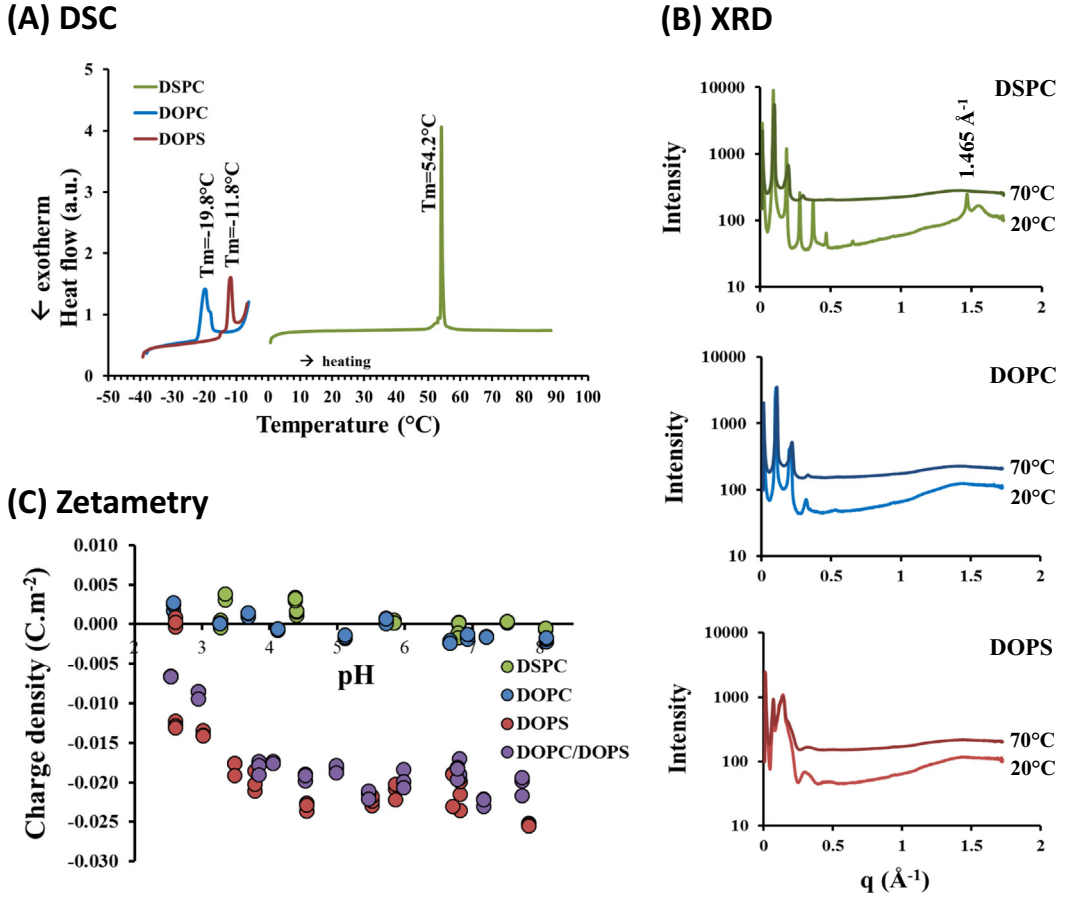

Fig. 3. Physical properties of bilayers of DSPC, DOPC and DOPS in PIPES/NaCl/0.1 mM $CaCl_2$ buffer at pH 6.7. (A) Determination of T_m by DSC upon heating MLVs at 2 °C·min^{-1}. (B) X-ray Scattering spectra of MLVs recorded at 20 or 70 °C at Wide (q > 1 Å^{-1}) and Small angles (q < 0.5 Å^{-1}). (C) Charge density of SUVs calculated from measurement of the zeta potential, ζ, at 20 °C, in PIPES/NaCl/0.1 mM $CaCl_2$ buffer at pH ranging from 2.5 to 8.

or DOPC dispersed in PIPES buffer at 20 °C, remained around 0 throughout the pH range investigated. Slightly negative values were found at the alkaline end, whereas slightly positive values were found at the acidic end, in accordance with increasing protonation (Fig. 3C). The corresponding zeta potential values, ζ, ranged from +5 to −4 mV from pH 2 to 8. In contrast, DOPS vesicles exhibited significant negative charge, with ζ values of −40 to −45 mV between pH 4.5 and 8, corresponding to σ of 2 to 2.5 × 10^{-2}C·m^{-2} (Fig. 3C). Equimolar mixtures of DOPS and DOPC produced vesicles with similar charge response as pure DOPS, indicating that the two lipids were mixed in the individual vesicles and that the larger absolute charge of DOPS overtook that of DOPC. In the literature, σ values of the order of 10^{-3} or 10^{-4}C·m^{-2} were reported for 1,2-dimyristoyl-*sn*-glycero-3-phosphocholine (DMPC) vesicles in presence of 25 or 100 mM NaCl, while the ζ values of DOPC, DMPC, DPPC or 1,2-dilaureoyl-*sn*-glycero-3-phosphocholine (DLPC) vesicles ranged from −5 to −10 mV depending on conditions [38,52,53]. Meanwhile, the ζ and σ values of DOPS moved to respectively −44 mV and −0.002 C·m^{-2} in water at pH ~ 6.7 (with Na^+ co-ions – [54,55]). Therefore, bilayers of DOPC, DOPS and DSPC varied in phase state (DOPC vs DSPC) or charge (DOPC vs DOPS) in PIPES buffer at pH 6.7 and at 20 °C.

3.3. Preferential adsorption of sodium caseinate on SLBs

3.3.1. Preferential adsorption of sodium caseinate onto the fluid phase of DSPC/DOPC bilayers

The interaction of sodium caseinate with DSPC/DOPC 50/50 mol% SLBs was investigated throughout time using AFM. These bilayers are composed of DSPC in the s_o phase and DOPC in the l_d phase at 20 °C, while both exhibit similar surface charge densities (Fig. 3). AFM images of the DSPC/DOPC 50/50 mol% SLBs clearly evidenced two phases, the thicker phase (Fig. 4A and C at $t = 0$) protruding by 1.21 ± 0.07 nm above the thinner phase. These two phases were respectively interpreted as the s_o DSPC-rich and the l_d DOPC-rich phases, in agreement with the increased thickness of bilayers when the acyl chains are fully stretched in their solid organization [56–58].

Within a short time (< 40 min; $N = 10$ independent observations) after injection of the sodium caseinate into the AFM sample cell, particles appeared to deposit onto the bilayers. The adsorption first occurred on the s_o/l_d phase boundary and on defects (holes) in the DOPC-rich l_d phase (compare images immediately before and after 21 min in Fig. 4A). The initially adsorbed casein particles were a few nm large and ~3 nm thick above the l_d phase (Fig. 4A, B), precise measurement of small deformable objects being difficult. Within completion of the next image, the area covered by the adsorbed casein particles seemed to grow (Fig. 4A), while the thickness of the adsorbed particles remained about 3 nm above the l_d phase (Fig. 4B). Then, the growing protein patches fused, up to forming a continuous layer over the l_d phase, 1.10 ± 0.15 nm higher than the DSPC-rich s_o-phase (Figs. 4B, 5A, E). No consistent time could be measured in this experiment, as injection of the sodium caseinate was performed at the side of the sample cell, at varying distance to the AFM probe, and without possible agitation. In conclusion, sodium caseinate adsorbed onto DSPC/DOPC 50/50 mol% supported bilayers where some disorder was present. That is, first, at the phase boundary and on hole defects present in the l_d phase, and second onto the whole l_d phase where larger molecular area opens space between the phospholipid molecules [16,57]. Coverage was also recorded onto pure DOPC bilayers, confirming this interpretation (Fig. SI-1).

The mechanical stability of the lipid bilayers was further evaluated using AFM force spectroscopy (AFM-FS). Upon applying normal force onto the bilayer with the AFM probe, local puncture may be achieved that clearly shows on the force curves as a typical breakthrough event ([59–61]; Fig. 5D). The corresponding breakthrough force value, F_b, has long been taken as indicative of the local mechanical stability of a given bilayer in specific environmental conditions [59,62].

F_b maps of DSPC/DOPC 50/50 mol% bilayers exhibited clear mechanical contrast. The DOPC-rich l_d phase ruptured at F_b of 5.9 ± 0.6 nN, while higher forces of 59.3 ± 1.0 nN were required to rupture the DSPC-rich s_o domains (Fig. 5B–C). This result agreed with previous findings [62,63]. Upon addition of the sodium caseinate, the F_b values observed on the still appearing l_d phase slightly decreased to 3.2 ± 0.7 nN. Where protein clusters had deposited, no breakthrough event was visible on the force curves (red pixels on Fig. 5B; D). Instead, the aspect of the force curves exhibited long-range interactions (Fig. 5D), possibly deformation of a soft polymer layer, as can be recorded over casein assemblies [64]. From the initial point of increasing force to the zero-separation segment of the force curves, a thickness of 19 ± 1 nm was measured over the caseinate clusters, versus 5.6 ± 0.4 nm for the s_o phospholipid domains and 5.2 ± 0.3 nm for the continuous l_d phospholipid phase ($N = 10$). Since caseinate was evaluated to be 1.1 nm thicker than the domains (Fig. 4), electrostatic repulsion between the AFM tip and the proteins probably also occurred. Overall, it seemed that the presence of adsorbed sodium caseinate altered the mechanical stability of the l_d phase, even at some distance to the actual interaction site, as discussed for protein-membrane interactions [65,66]. It is also possible that casein peptides, which may be present in caseinate either naturally (from milk) or as a result of caseinate production using alkali, penetrate into the l_d phase and alter the lateral packing of the phospholipid [67]. Finally, the mechanical stability of the s_o phase after incubation of the bilayers in presence of caseinate did not significantly change, with F_b values of 52 ± 10 nN (Fig. 5B–C). This result confirmed that the protein particles did not interfere with the DSPC-rich s_o-phase.

Early studies using electron microscopy images of co-compressed phospholipid monolayers and milk proteins showed that β-casein or the whey protein β-lactoglobulin (β-lg) preferably interacted with phospholipids in the liquid-expanded phase rather than onto liquid-condensed (or s_o) phases [15,68], in agreement with the general picture [69,70]. Later, DLS was used to measure variation of the diameter of liposomes in presence of milk proteins. Interaction of β-casein, α_{s1}-casein or κ-casein with liposomes of two different phospholipids in l_d phase was reported, although it depended on specific ionic conditions [71]. In contrast, no interaction was found between sodium caseinate and egg-PC (mainly 1-stearoyl,2-oleoyl-*sn*-glycero-3-phosphocholine) or between sodium caseinate and DPPC vesicles, neither in their l_d nor in their s_o phase [22,72]. To the authors' knowledge, only the interaction of β-casein with phospholipid monolayers was investigated in detail. In these studies, β-casein and the phospholipid film were compressed together in a Langmuir trough, which is a relevant model rather for emulsification than for protein-membrane interaction. In this approach, penetration of the β-casein increases molecular area of the phospholipids, thereby showing low miscibility [29,73,74]. The β-casein and phospholipid co-exist at the interface for low initial pressures of the lipid film, exhibiting complex organization(s). Results indicate that β-casein can interact with gaseous or liquid-expanded lipid phases but also, in specific conditions, with liquid-condensed (LC) lipid domains due to the higher density for electrostatic pairing [27–29,74]. However, if the initial pressure exceeds 18 mN·m^{-1}, β-casein is not able to penetrate the already constituted LC phase or is squeezed out the compressed film [28,73,74] and remains adsorbed onto it [27,73].

If initial adsorption of the sodium caseinate particles is driven at least by hydrophobic interactions, marked by the attraction for bilayer edges and height mismatch, cooperative adsorption is clearly also at play, as revealed by the lateral and rapid growth of the protein clusters, up to complete coverage (Figs. 4A, C). Cooperative adsorption, defined as the enhanced adsorption where already adsorbed protein is present, has also been reported for e.g. ezrin on 1-palmitoyl,2-oleoyl-*sn*-glycero-3-phosphocholine (POPC) bilayers [75] or for annexin V crystals on DOPC/DOPS membranes [76]. In different thermodynamic approaches, attempts were made to describe cooperative adsorption [18]. In a first model, the adsorbing protein would experience either deposition onto

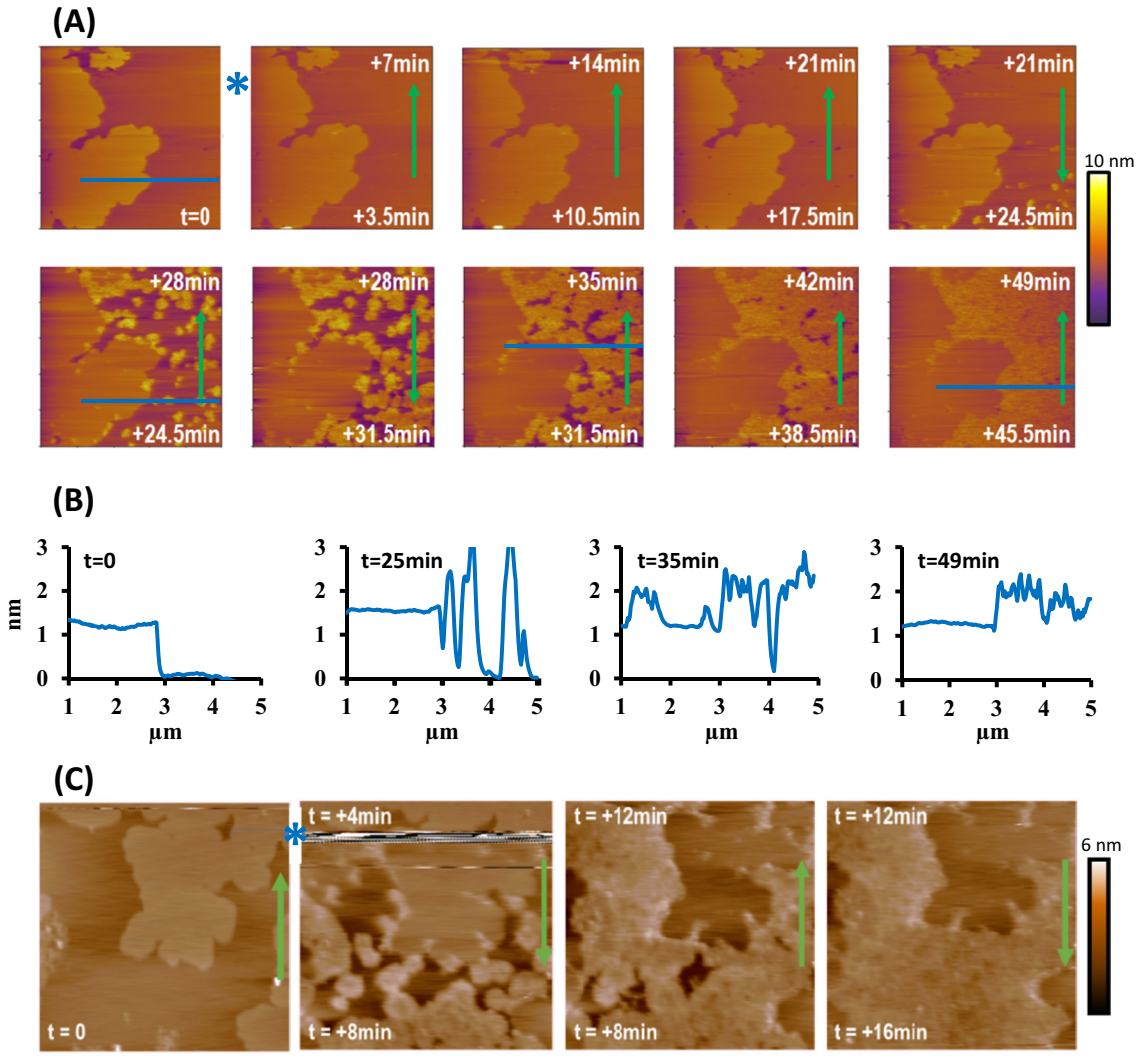

Fig. 4. Interaction of sodium caseinate with DSPC/DOPC 50/50 mol% SLBs in PIPES/NaCl/0.1 mM $CaCl_2$ buffer at pH 6.7 and at 20 °C. (A) and (C) fully independent typical time series of AFM 5 × 5 µm^2 topographical images prior to (t = 0) and after ($t > 0$) injection of 50 µg of sodium caseinate (indicated with the blue star symbol). Arrows indicate the slow scan direction for each image. (B) Cross sections of the images, identified by the approximate timing, where indicated by the blue lines in (A). Images in (A) were obtained in contact mode; images in (C) were obtained in AC mode.

the surface, followed by lateral diffusion and accretion to the already present protein cluster, or deposition onto the protein cluster and insertion, or rejection [75,77]. Each protein behavior would result from the balance between these three ways. More recently, Rabe et al. [78] proposed that bulk protein, when it approaches an already adsorbed protein cluster, is tracked to the nearest available binding site, i.e. to the edge of the cluster, providing that it can be found within a certain distance called the "cooperative radius". If not, the protein is rejected into the bulk [78]. This model accounts for the heterogeneous coverage of the bilayer by the protein, marked by large clusters, as observed in Fig. 4. It would also account for the lateral accretion of sodium caseinate particles that are otherwise repulsive to each other, being electronegative (Fig. 2). Finally, it was suggested that recruitment of specific phospholipids by the adsorbing protein could induce cooperative adsorption through lipid-lipid separation [79], which is unlikely in the present case where mainly DOPC is present in the l_d phase of the bilayers.

3.3.2. Net negative surface charge of DOPC/DOPS bilayers tends to delay adsorption of sodium caseinate

In this experiment, the interaction of sodium caseinate with DOPC/DOPS 50/50 mol% SLBs was investigated, where DOPC and DOPS respectively bore a net neutral and a negative surface charge at pH 6.7 and at 20 °C (Fig. 3). The DOPC/DOPS 50/50 mol% SLBs exhibited different organizations, thereby indicating their metastable nature. Noteworthy, imaging of these fluid bilayers could reveal difficult, where the sometimes-evidenced domains appeared to fluctuate in shape. Domains often appeared in presence of 0.1 mM $CaCl_2$, as expected ([34]; Fig. 6), and sometimes in absence of calcium ions. No domain was visible in presence of 2 mM $CaCl_2$ (Obeid, personal communication; [76]). Calcium ions therefore contribute to the miscibility of PS and PC phospholipids, although conclusions differ [80–82]. These domains protruded above the continuous phase by a height step of only 0.2–0.67 nm (± 0.11 nm) depending on preparation. In contrast, they were clearly visible in friction, despite their comparable l_d phase state. According to the observations by Ross et al. [34], domains were supposed to be adhesive DOPS-rich clusters while the continuous phase was DOPC-rich with dispersed DOPS.

When cracks or defects were present in the DOPC/DOPS bilayers, the injected sodium caseinate readily associated with them, but did not adsorb on the bilayer itself (Fig. 6A, $N = 5$ independent observations). When the bilayers showed no phase separation or numerous small dispersed domains, adsorption of the caseinate seemed not to occur, or not to occur before extended times > 1 h (Fig. 6A, B, N = 5

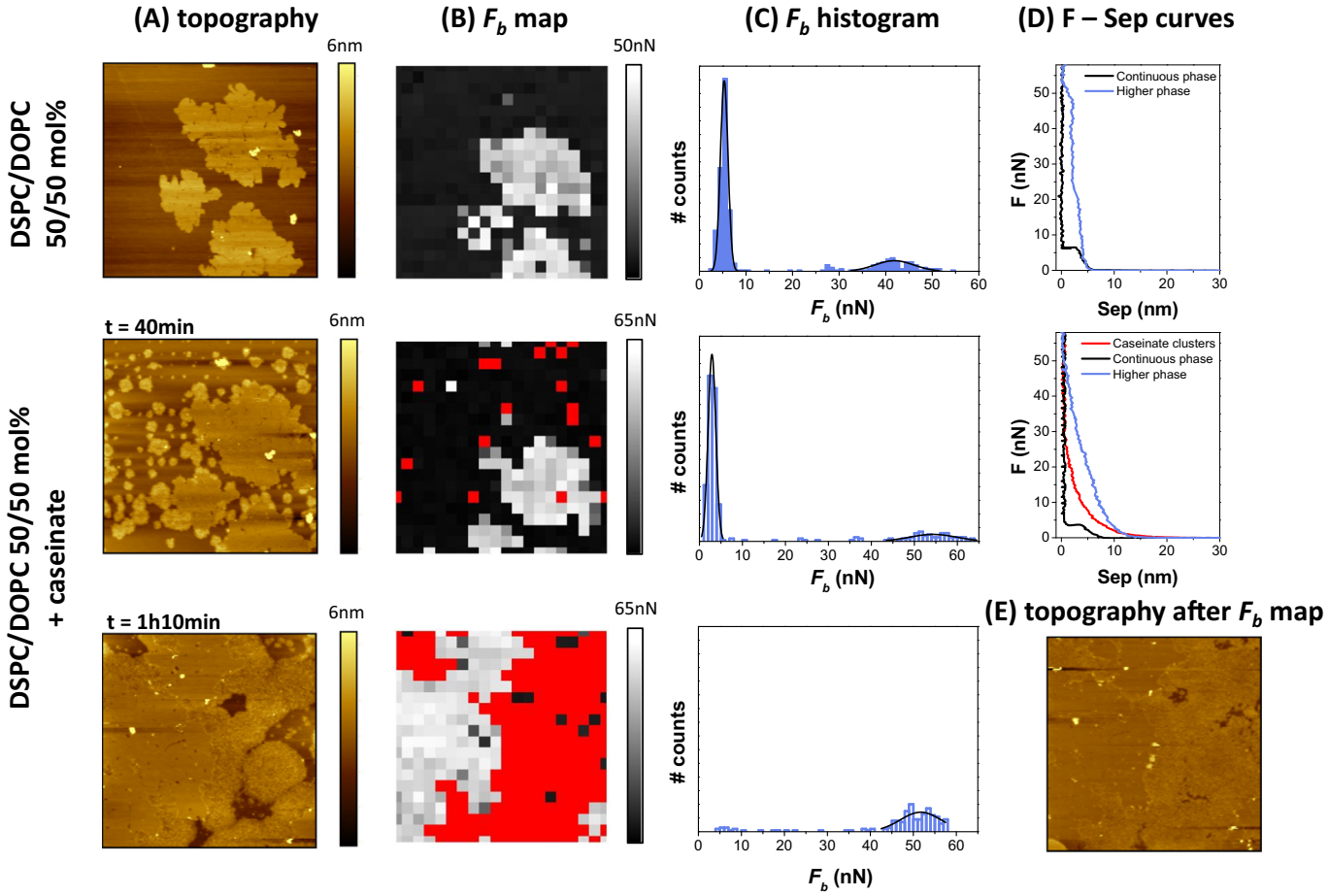

Fig. 5. Change in mechanical stability of DSPC/DOPC 50/50 mol% bilayers as a consequence of adsorption of sodium caseinate, measured by AFM-FS in PIPES/NaCl/0.1 mM $CaCl_2$ buffer at pH 6.7 and at 20 °C. (A) AC mode topography over 8 × 8 μm^2, (B) corresponding F_b maps, (C) F_b histogram and (D) typical force-separation curves recorded prior to (upper row) or after incubation for 40 min (middle row) or for 1 h10 min (bottom row) in presence of sodium caseinate. (E) A different location (5 × 5 μm^2) after performing the F_b map. Red pixels on the F_b maps indicate the absence of a breakthrough event.

independent observations). The thickness of the protein layer was 1–4 nm, where it was possible to be measured. Finally, when the bilayers showed phase separation, with rather large domains, adsorption of the sodium caseinate occurred within minutes onto the continuous phase, up to full coverage (Fig. 6C, D, $N = 3$ independent observations) and the thickness of the protein layer reached up to 8 nm.

Prior to injection of the sodium caseinate, the F_b maps of DOPC/DOPS 50/50 mol% SLBs exhibited homogenous F_b values of 3.9 ± 0.9 nN, while lower forces of 2.9 ± 1.1 nN sufficed to rupture the bilayers once protein had adsorbed, in places where the bilayer is still visible (Fig. 7A–C). In agreement with what was observed for DSPC/DOPC 50/50 mol% SLBs (Fig. 5), the adsorbed sodium caseinate destabilized the underlying membrane. In places already covered with sodium caseinate, no rupture event and deformation of soft material were observed on the force curves (Fig. 7D), as previously observed (Fig. 5D).

In conclusion, sodium caseinate did not adsorb homogeneously onto the surface of DOPC/DOPS 50/50 mol% bilayers, in spite of their homogeneous l_d phase state. Instead, sodium caseinate did not seem to adsorb onto the DOPS-rich domains, when phase separation was present, and the presence of dispersed DOPS in the bilayers seemed to delay adsorption onto the mixed bilayers. Electrostatic repulsion between the negative DOPS surface and negative sodium caseinate particles probably accounts for these observations, even though low dielectric constant near the surface of the membrane may slightly increase the pI of the sodium caseinate [83]. Another reason for the better adsorption of sodium caseinate onto DOPC rather than DOPS could be their different molecular area, hence variable inter-molecular space for protein penetration [47]. Using dipalmitoyl phospholipids, Garcia-Manyes et al. [62] reported that a significantly greater force was required to break through a PS bilayer, compared with PC.

In the literature, dependence of the adsorption of casein proteins or casein particles onto charge is however unclear. At pH 7, sodium caseinate particles were reported not to adsorb neither onto egg-phosphatidylcholine (1-stearoyl,2-oleoyl-*sn*-glycero-3-phosphocholine) nor onto DPPC [22,72]. In contrast, some binding of casein particles, κ-casein, α_s-casein or β-casein onto DMPC or egg-PC vesicles was reported when NaCl was present in neutral buffer [6,71]. In these conditions, caseins furthermore showed greater affinity for negatively charged phosphatidylglycerol (PG) bilayers, in contrast to our results. At pH 9 where β-casein is largely negatively charged, repulsive electrostatic interaction can hinder penetration of the protein in co-compressed β-casein and DPPC Langmuir films [74,84]. However, these reports lack direct observation of the casein-membrane interaction [71].

3.4. Relevance of phase and charge upon interaction of casein particles with membranes

In-situ observation of the interaction between dispersed sodium caseinate particles and phospholipid bilayers in hydrated conditions showed that casein particles interacted with bilayers in their l_d state, in contrast with s_o-phase bilayers where compact lateral organization of the phospholipids probably prevents penetration of the protein.

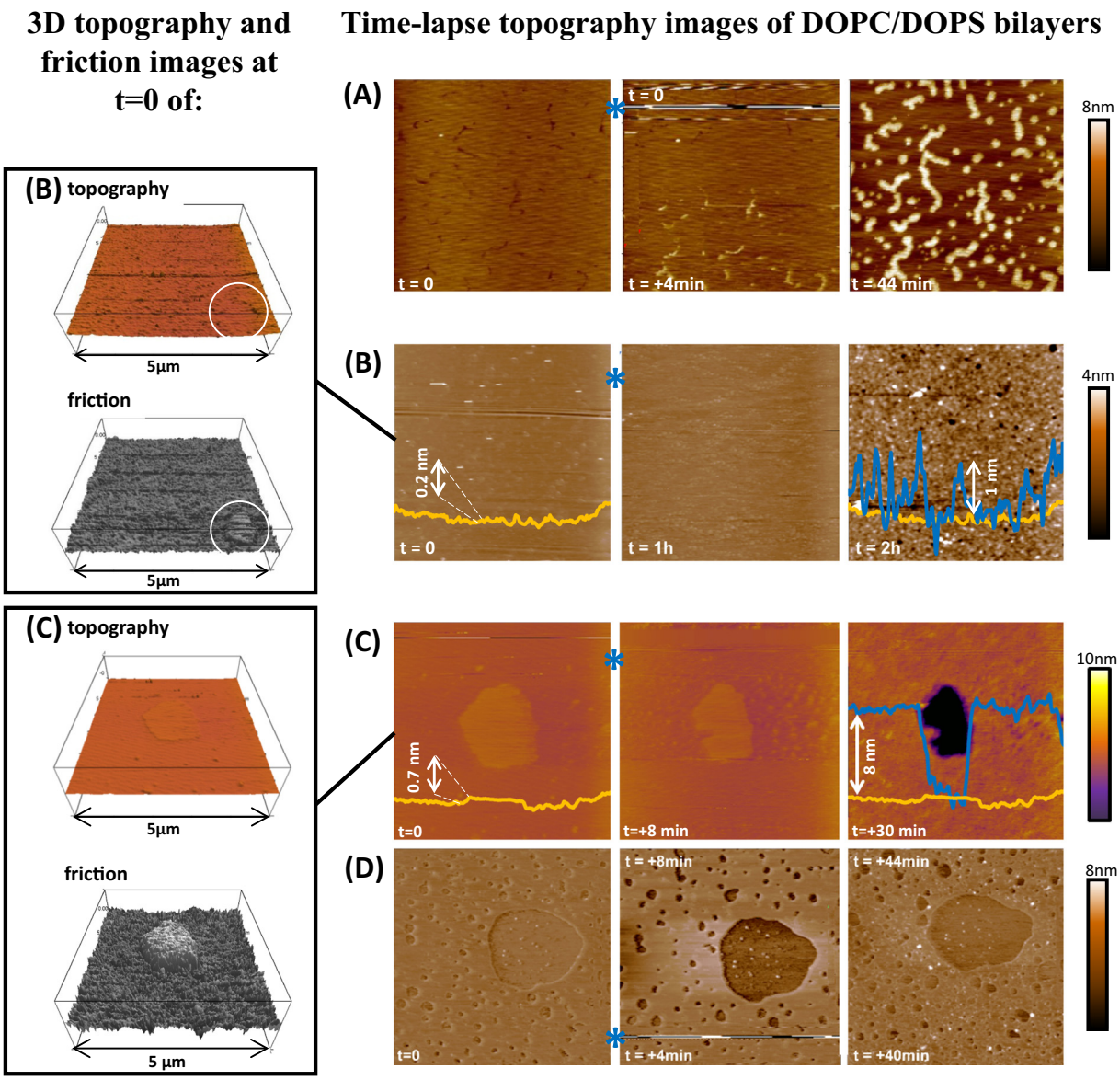

Fig. 6. Interaction of sodium caseinate with DOPC/DOPS 50/50 mol% bilayers in PIPES/NaCl/0.1 mM $CaCl_2$ buffer at pH 6.7 and at 20 °C. The right panel shows typical time series of AFM 5 × 5 µm^2 topographical images prior to ($t = 0$) and after ($t > 0$) injection of 50 µg of sodium caseinate (indicated with the blue star symbol). (A) Homogeneous bilayer where incomplete SLB formation left cracks: sodium caseinate clearly deposited in the cracks (white strands at $t = 44$ min) but not on the bilayer. (B) Near homogeneous bilayers where small, dispersed domains were visible. (C–D) Fully independent (distinct facilities and operators) examples of DOPC/DOPS 50/50 mol% bilayers with separated domains. On the left panel, 3D-reconstitutions of images B and C at t = 0 show that these domains were barely visible in topography, but highly contrasted in friction (one large domain is shown in the white circle). In time series B and C, the yellow trace is the cross-section taken approximately at the half of the image at t = 0, while the blue trace is the same cross-section after deposition of the sodium caseinate. They are superimposed in the last image of each series, for better comparison. Images in A, B, D were obtained with AC mode; images in C were obtained in contact mode.

Furthermore, electrostatic repulsion by PS seemed to inhibit adsorption of the sodium caseinate, even though the bilayer was in the l_d phase (Fig. 8). This modulation of adsorption of casein particles by modulation of the polar lipid composition of the membrane could be a key issue of their traffic throughout the lactating cell's organelles and membrane. While the polar lipid compositions of the ER and the Golgi membranes seem quantitatively similar [85], the former and latter bear symmetric and asymmetric leaflets, respectively [86]. Typically, the negative PS, phosphatidylethanolamines (PE) and phosphatidylinositols (PI) are rather found on the cytosolic leaflet of the Golgi membrane, and PC and sphingomyelin on the luminal leaflet, i.e. like for the plasma membrane [86,87]. Whether or not the Golgi vesicles maintain this asymmetry is unclear, but the repulsive/attractive property of the inner leaflet could be important when carrying the casein micelles prior to secretion into the lactating duct. The same holds true for the ER-to-Golgi transport, where this time adsorption of the casein to membrane is seeked to secure transport [5].

Another interesting issue of the present results is the possible impact of the lateral distribution of the polar lipids within the membrane, on the modulation of its repulsive/attractive interaction with sodium caseinate particles. Fig. 6 indeed suggested that when DOPS was homogeneously mixed with DOPC, or when it was dispersed into small scattered domains, binding and spreading of casein clusters onto the DOPC/DOPS 50/50 mol% bilayers was somewhat inhibited. Only when DOPS was recruited and clustered into domains, the net negative phase of the continuous phase was sufficiently neutralized to allow interaction with the caseinate. This observation was in line with the proposition that electrostatic interaction and cooperative adsorption are important

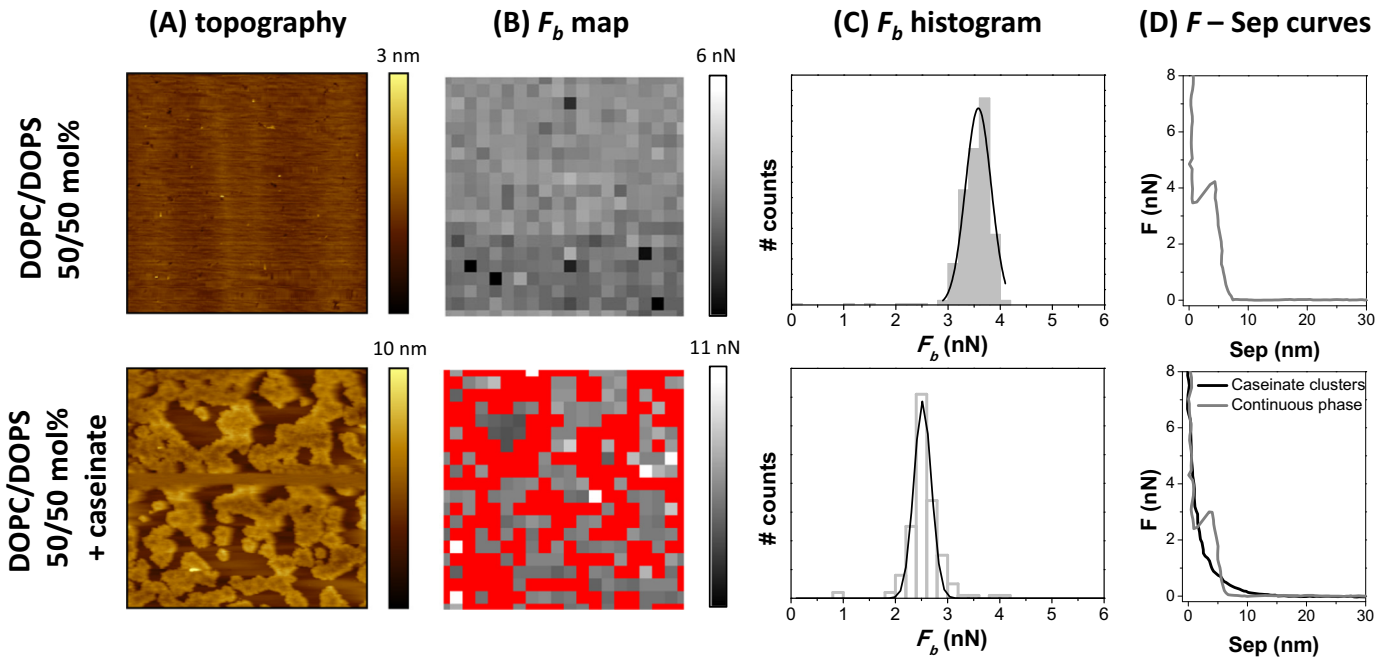

Fig. 7. Change in mechanical stability of DOPC/DOPS 50/50 mol% SLBs as a consequence of adsorption of sodium caseinate, measured by AFM-FS in PIPES/NaCl/0.1 mM $CaCl_2$ buffer at pH 6.7 and at 20 °C. (A) AC mode topography over 5 × 5 μm^2, (B) corresponding F_b maps, (C) F_b histogram and (D) typical force-separation curves recorded prior to (upper row) or after 40 min incubation with sodium caseinate (bottom row). Red pixels on the F_b maps indicate the absence of a breakthrough event.

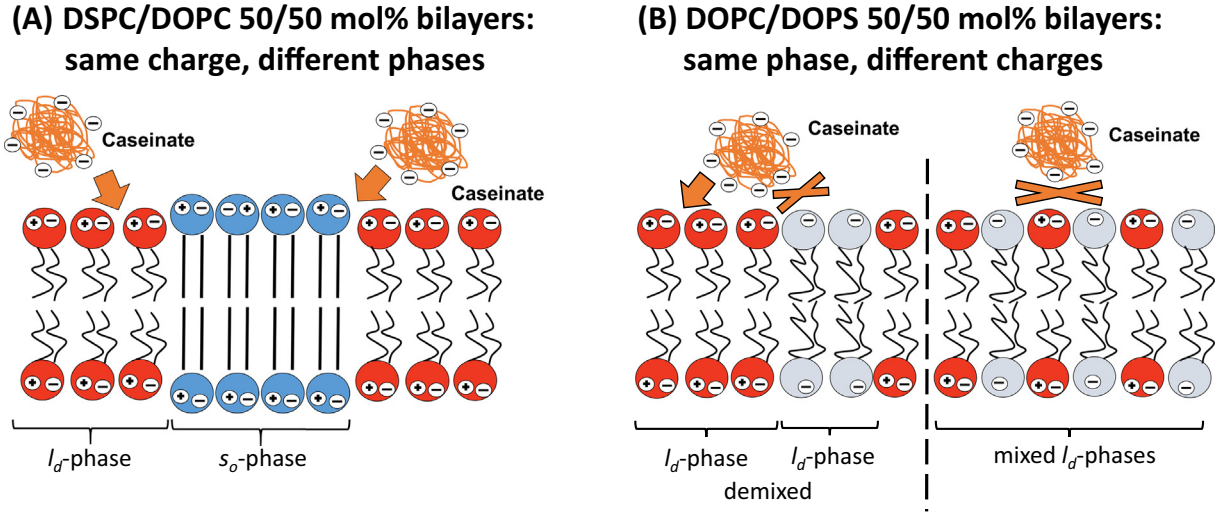

Fig. 8. Interaction of sodium caseinate particles with hydrated phospholipid bilayers in PIPES/NaCl/0.1 mM $CaCl_2$ buffer at pH 6.7 and at 20 °C. (A) DSPC/DOPC 50/50 mol%: the bilayers exhibit s_o-l_d phase separation and the caseinate particles adsorb only on the l_d phase where inter-molecular distance is higher than in the s_o phase. (B) DOPC/DOPS 50/50 mol%: the bilayers exhibit l_d-l_d phase separation and the casein particles adsorb only onto the DOPC-rich phase where net electrostatic repulsion is sufficiently reduced compared to that of the DOPS-rich domains or DOPC/DOPS mixed phase.

mechanisms to direct the behavior of casein particles when they approach lipid membranes. The role of calcium ions in the segregation of PS phospholipids from PC ones remains to be elucidated.

These results provide new insight on the mechanisms that drive interaction of the casein particles with phospholipid membranes, with possible implication for a better understanding of the synthesis of the casein micelle. Furthermore, interaction between the mature casein micelle and the membrane of the milk fat globule is susceptible to occur in the secreted milk itself, during storage, digestion or dairy processes such as coagulation or homogenization [88,89].

4. Conclusion

The use of AFM imaging and force spectroscopy combined with sample stages accomodating liquid samples and in-situ modification of the aqueous bulk have permitted the direct observation of the interaction of casein particle with various types of phospholipid bilayers. Sodium caseinate particles could not adsorb onto phospholipids in the s_o phase. In contrast, they adsorbed onto the l_d phase, providing that no significant electrostatic repulsion was present. This report illustrates the interest of AFM imaging and force spectroscopy to provide qualitative, direct observation data on protein-membrane interactions.

Conflict of interest

Authors declare no conflict of interest. All funders of the research are mentioned in the Acknowledgement section of the Manuscript.

Transparency document

The Transparency document associated with this article can be found in the online version.

Acknowledgements

Sameh Obeid (INRA STLO) is thanked for fruitful discussion on AFM imaging of protein-membrane interactions. CEPIA, INRA financially supported Adrián Crespo-Villanueva and the presented research under the grant 2016-2017 AIC-P2B (PI Fanny Guyomarc'h). We acknowledge financial support from the Generalitat de Catalunya (AGAUR 2017 SG 1442) and Spanish Ministry of Economy and Competitiveness (MINECO) and FEDER (CTQ2015-66194-R MINECO/FEDER) projects, and Instituto de Salud Carlos III, through “Acciones CIBER”. The Asylum Research MFP 3D-BIO atomic force microscope at STLO was funded by the European Union (FEDER), the French Ministry of Education and Research, INRA, Conseil Général 35 and Rennes Métropole.

Appendix A. Supplementary data

Supplementary data to this article can be found online at https://doi.org/10.1016/j.bbamem.2018.09.016.

References

[1] C. Broyard, F. Gaucheron, Modifications of structures and functions of caseins: a scientific and technological challenge, Dairy Sci. Technol. 95 (2016) 831–862, https://doi.org/10.1007/s13594-015-0220-y.
[2] H.M. Farrell, R. Jimenez-Flores, G.T. Bleck, E.M. Brown, J.E. Butler, L.K. Creamer, C.L. Hicks, C.M. Hollar, K.F. Ng-Kwai-Hang, H.E. Swaisgood, Nomenclature of the proteins of cows' milk—sixth revision, J. Dairy Sci. 87 (2004) 1641–1674, https://doi.org/10.3168/jds.S0022-0302(04)73319-6.
[3] H.M. Farrell, E.L. Malin, E.M. Brown, P.X. Qi, Casein micelle structure: what can be learned from milk synthesis and structural biology? Curr. Opin. Colloid Interface Sci. 11 (2006) 135–147, https://doi.org/10.1016/j.cocis.2005.11.005.
[4] Y. Clermont, L. Xia, A. Rambourg, J.D. Turner, L. Hermo, Transport of casein submicelles and formation of secretion granules in the Golgi apparatus of epithelial cells of the lactating mammary gland of the rat, Anat. Rec. 235 (1993) 363–373, https://doi.org/10.1002/ar.1092350305.
[5] A. Le Parc, J. Leonil, E. Chanat, αS1-casein, which is essential for efficient ER-to-Golgi casein transport, is also present in a tightly membrane-associated form, BMC Cell Biol. 11 (2010) 65, https://doi.org/10.1186/1471-2121-11-65.
[6] M. Sokolovski, T. Sheynis, S. Kolusheva, R. Jelinek, Membrane interactions and lipid binding of casein oligomers and early aggregates, Biochim. Biophys. Acta Biomembr. 1778 (2008) 2341–2349, https://doi.org/10.1016/j.bbamem.2008.07.001.
[7] A. Mulgrew-Nesbitt, K. Diraviyam, J. Wang, S. Singh, P. Murray, Z. Li, L. Rogers, N. Mirkovic, D. Murray, The role of electrostatics in protein–membrane interactions, Biochim. Biophys. Acta BBA - Mol. Cell Biol. Lipids 1761 (2006) 812–826, https://doi.org/10.1016/j.bbalip.2006.07.002.
[8] A.H. Juffer, C.M. Shepherd, H.J. Vogel, Protein–membrane electrostatic interactions: application of the Lekner summation technique, J. Chem. Phys. 114 (2001) 1892–1905, https://doi.org/10.1063/1.1334901.
[9] G. Lindblom, P.-O. Quist, Protein and peptide interactions with lipids: structure, membrane function and new methods, Curr. Opin. Colloid Interface Sci. 3 (1998) 499–508, https://doi.org/10.1016/S1359-0294(98)80024-1.
[10] T. Cserháti, M. Szögyi, Interaction of phospholipids with proteins, peptides and amino acids. New advances 1987–1989, Int. J. BioChemiPhysics 23 (1991) 131–145, https://doi.org/10.1016/0020-711X(91)90181-L.
[11] D. Needham, T.J. McIntosh, S.A. Simon, D. Zhelev, Adsorption, molecular exchange and defect formation in membranes, Curr. Opin. Colloid Interface Sci. 3 (1998) 511–517, https://doi.org/10.1016/S1359-0294(98)80026-5.
[12] D. Asthagiri, A.M. Lenhoff, Influence of structural details in modeling electrostatically driven protein adsorption, Langmuir 13 (1997) 6761–6768, https://doi.org/10.1021/la970608u.
[13] V.P. Zhdanov, B. Kasemo, Van der Waals interaction during protein adsorption on a solid covered by a thin film, Langmuir 17 (2001) 5407–5409, https://doi.org/10.1021/la0104222.
[14] K. Glasmästar, C. Larsson, F. Höök, B. Kasemo, Protein adsorption on supported phospholipid bilayers, J. Colloid Interface Sci. 246 (2002) 40–47, https://doi.org/10.1006/jcis.2001.8060.
[15] D.G. Cornell, R.J. Carroll, Electron microscopy of lipid-protein monolayers, Colloids Surf. A Physicochem. Eng. Asp. 6 (1983) 385–393, https://doi.org/10.1016/0166-6622(83)80029-8.
[16] A. Alessandrini, P. Facci, Unraveling lipid/protein interaction in model lipid bilayers by atomic force microscopy, J. Mol. Recognit. 24 (2011) 387–396, https://doi.org/10.1002/jmr.1083.
[17] S.A. Sánchez, M.A. Tricerri, G. Ossato, E. Gratton, Lipid packing determines protein–membrane interactions: challenges for apolipoprotein A-I and high density lipoproteins, Biochim. Biophys. Acta Biomembr. 1798 (2010) 1399–1408, https://doi.org/10.1016/j.bbamem.2010.03.019.
[18] C. Steinem, A. Janshoff, Multicomponent membranes on solid substrates: interfaces for protein binding, Curr. Opin. Colloid Interface Sci. 15 (2010) 479–488, https://doi.org/10.1016/j.cocis.2010.06.004.
[19] M. Edvardsson, S. Svedhem, G. Wang, R. Richter, M. Rodahl, B. Kasemo, QCM-D and reflectometry instrument: applications to supported lipid structures and their biomolecular interactions, Anal. Chem. 81 (2009) 349–361, https://doi.org/10.1021/ac801523w.
[20] R. Mendelsohn, G. Mao, C.R. Flach, Infrared reflection–absorption spectroscopy: principles and applications to lipid–protein interaction in Langmuir films, Biochim. Biophys. Acta Biomembr. 1798 (2010) 788–800, https://doi.org/10.1016/j.bbamem.2009.11.024.
[21] A. Blume, A. Kerth, Peptide and protein binding to lipid monolayers studied by FT-IRRA spectroscopy, Biochim. Biophys. Acta Biomembr. 1828 (2013) 2294–2305, https://doi.org/10.1016/j.bbamem.2013.04.014.
[22] Y. Fang, D.G. Dalgleish, Studies on interactions between phosphatidylcholine and casein, Langmuir 11 (1995) 75–79, https://doi.org/10.1021/la00001a016.
[23] S. Morandat, K. El Kirat, Real-time atomic force microscopy reveals cytochrome c-induced alterations in neutral lipid bilayers, Langmuir 23 (2007) 10929–10932, https://doi.org/10.1021/la702158j.
[24] O. Freudenthal, F. Quilès, G. Francius, K. Wojszko, M. Gorczyca, B. Korchowiec, E. Rogalska, Nanoscale investigation of the interaction of colistin with model phospholipid membranes by Langmuir technique, and combined infrared and force spectroscopies, Biochim. Biophys. Acta Biomembr. 1858 (2016) 2592–2602, https://doi.org/10.1016/j.bbamem.2016.07.015.
[25] D.E. Saslowsky, J. Lawrence, X. Ren, D.A. Brown, R.M. Henderson, J.M. Edwardson, Placental alkaline phosphatase is efficiently targeted to rafts in supported lipid bilayers, J. Biol. Chem. 277 (2002) 26966–26970, https://doi.org/10.1074/jbc.M204669200.
[26] P.-E. Milhiet, F. Gubellini, A. Berquand, P. Dosset, J.-L. Rigaud, C. Le Grimellec, D. Lévy, High-resolution AFM of membrane proteins directly incorporated at high density in planar lipid bilayer, Biophys. J. 91 (2006) 3268–3275, https://doi.org/10.1529/biophysj.106.087791.
[27] S. Gallier, D. Gragson, R. Jiménez-Flores, D.W. Everett, Surface characterization of bovine milk phospholipid monolayers by Langmuir isotherms and microscopic techniques, J. Agric. Food Chem. 58 (2010) 12275–12285, https://doi.org/10.1021/jf102185a.
[28] A. Lucero Caro, M.R. Rodríguez Niño, J.M. Rodríguez Patino, Topography of dipalmitoyl-phosphatidyl-choline monolayers penetrated by β-casein, Colloids Surf. A Physicochem. Eng. Asp. 346 (2009) 146–157, https://doi.org/10.1016/j.colsurfa.2009.06.007.
[29] C. Berton-Carabin, C. Genot, C. Gaillard, D. Guibert, M.H. Ropers, Design of interfacial films to control lipid oxidation in oil-in-water emulsions, Food Hydrocoll. 33 (2013) 99–105, https://doi.org/10.1016/j.foodhyd.2013.02.021.
[30] M. Panouillé, T. Nicolai, D. Durand, Heat induced aggregation and gelation of casein submicelles, Int. Dairy J. 14 (2004) 297–303, https://doi.org/10.1016/j.idairyj.2003.09.003.
[31] W. Nash, D. Pinder, Y. Hemar, H. Singh, Dynamic light scattering investigation of sodium caseinate and xanthan mixtures, Int. J. Biol. Macromol. 30 (2002) 269–271, https://doi.org/10.1016/S0141-8130(02)00041-7.
[32] B. Chu, Z. Zhou, G. Wu, H.M. Farrell, Laser light scattering of model casein solutions: effects of high temperature, J. Colloid Interface Sci. 170 (1995) 102–112, https://doi.org/10.1006/jcis.1995.1077.
[33] P. Qu, G. Gésan-Guiziou, A. Bouchoux, Dead-end filtration of sponge-like colloids: the case of casein micelle, J. Membr. Sci. 417–418 (2012) 10–19, https://doi.org/10.1016/j.memsci.2012.06.003.
[34] M. Ross, C. Steinem, H.-J. Galla, A. Janshoff, Visualization of chemical and physical properties of calcium-induced domains in DPPC/DPPS Langmuir – Blodgett layers, Langmuir 17 (2001) 2437–2445, https://doi.org/10.1021/la001617x.
[35] E. Prenner, M. Chiu, Differential scanning calorimetry: an invaluable tool for a detailed thermodynamic characterization of macromolecules and their interactions, J. Pharm. Bioallied Sci. 3 (2011) 39, https://doi.org/10.4103/0975-7406.76463.
[36] T. Bizien, J.-C. Ameline, K.G. Yager, V. Marchi, F. Artzner, Self-organization of quantum rods induced by lipid membrane corrugations, Langmuir 31 (2015) 12148–12154, https://doi.org/10.1021/acs.langmuir.5b03335.
[37] T.N. Blanton, C.L. Barnes, M. Lelental, Preparation of silver behenate coatings to provide low- to mid-angle diffraction calibration, J. Appl. Crystallogr. 33 (2000) 172–173, https://doi.org/10.1107/S0021889899012388.
[38] S. Garcia-Manyes, G. Oncins, F. Sanz, Effect of temperature on the nanomechanics of lipid bilayers studied by force spectroscopy, Biophys. J. 89 (2005) 4261–4274, https://doi.org/10.1529/biophysj.105.065581.
[39] M.-P. Mingeot-Leclercq, M. Deleu, R. Brasseur, Y.F. Dufrêne, Atomic force microscopy of supported lipid bilayers, Nat. Protoc. 3 (2008) 1654–1659, https://doi.org/10.1038/nprot.2008.149.
[40] D.G. Dalgleish, Measurement of electrophoretic mobilities and zeta-potentials of

particles from milk using laser Doppler electrophoresis, J. Dairy Res. 51 (1984) 425–438.
[41] D.F. Darling, J. Dickson, The determination of the zeta potential of casein micelles, J. Dairy Res. 46 (1979) 329, https://doi.org/10.1017/S0022029900017258.
[42] S. Mezdour, J. Korolczuck, Zeta potential of sodium caseinate in water-ethanol solutions, Milchwissenschaft 65 (2010) 392–395.
[43] H. Ma, P. Forssell, R. Partanen, R. Seppänen, J. Buchert, H. Boer, Sodium caseinates with an altered isoelectric point as emulsifiers in oil/water systems, J. Agric. Food Chem. 57 (2009) 3800–3807, https://doi.org/10.1021/jf803104s.
[44] R. Koynova, M. Caffrey, Phases and phase transitions of the phosphatidylcholines, Biochim. Biophys. Acta Rev. Biomembr. 1376 (1998) 91–145, https://doi.org/10.1016/S0304-4157(98)00006-9.
[45] T.P.W. McMullen, R.N. McElhaney, Differential scanning calorimetric studies of the interaction of cholesterol with distearoyl and dielaidoyl molecular species of phosphatidylcholine, phosphatidylethanolamine, and phosphatidylserine, Biochemistry (Mosc) 36 (1997) 4979–4986, https://doi.org/10.1021/bi962815j.
[46] C. Galvagnion, J.W.P. Brown, M.M. Ouberai, P. Flagmeier, M. Vendruscolo, A.K. Buell, E. Sparr, C.M. Dobson, Chemical properties of lipids strongly affect the kinetics of the membrane-induced aggregation of α-synuclein, Proc. Natl. Acad. Sci. 113 (2016) 7065–7070, https://doi.org/10.1073/pnas.1601899113.
[47] H.I. Petrache, S. Tristram-Nagle, K. Gawrisch, D. Harries, V.A. Parsegian, J.F. Nagle, Structure and fluctuations of charged phosphatidylserine bilayers in the absence of salt, Biophys. J. 86 (2004) 1574–1586, https://doi.org/10.1016/S0006-3495(04)74225-3.
[48] J. Valério, M.H. Lameiro, S.S. Funari, M.J. Moreno, E. Melo, Temperature effect on the bilayer stacking in multilamellar lipid vesicles, J. Phys. Chem. B 116 (2012) 168–178, https://doi.org/10.1021/jp206848u.
[49] J. Stümpel, H. Eibl, A. Nicksch, X-ray analysis and calorimetry on phosphatidylcholine model membranes. The influence of length and position of acyl chains upon structure and phase behaviour, Biochim. Biophys. Acta Biomembr. 727 (1983) 246–254, https://doi.org/10.1016/0005-2736(83)90410-8.
[50] B. Gumí-Audenis, L. Costa, L. Redondo-Morata, P.-E. Milhiet, F. Sanz, R. Felici, M.I. Giannotti, F. Carlà, In-plane molecular organization of hydrated single lipid bilayers: DPPC:cholesterol, Nanoscale 10 (2018) 87–92, https://doi.org/10.1039/C7NR07510C.
[51] R. Zantl, L. Baicu, F. Artzner, I. Sprenger, G. Rapp, J.O. Rädler, Thermotropic phase behavior of cationic lipid − DNA complexes compared to binary lipid mixtures, J. Phys. Chem. B 103 (1999) 10300–10310, https://doi.org/10.1021/jp991596j.
[52] S. Garcia-Manyes, G. Oncins, F. Sanz, Effect of pH and ionic strength on phospholipid nanomechanics and on deposition process onto hydrophilic surfaces measured by AFM, Electrochim. Acta 51 (2006) 5029–5036, https://doi.org/10.1016/j.electacta.2006.03.062.
[53] L. Redondo-Morata, G. Oncins, F. Sanz, Force spectroscopy reveals the effect of different ions in the nanomechanical behavior of phospholipid model membranes: the case of potassium cation, Biophys. J. 102 (2012) 66–74, https://doi.org/10.1016/j.bpj.2011.10.051.
[54] C. Lütgebaucks, C. Macias-Romero, S. Roke, Characterization of the interface of binary mixed DOPC:DOPS liposomes in water: the impact of charge condensation, J. Chem. Phys. 146 (2017) 044701, , https://doi.org/10.1063/1.4974084.
[55] M.C. Smith, R.M. Crist, J.D. Clogston, S.E. McNeil, Zeta potential: a case study of cationic, anionic, and neutral liposomes, Anal. Bioanal. Chem. 409 (2017) 5779–5787, https://doi.org/10.1007/s00216-017-0527-z.
[56] K. El Kirat, S. Morandat, Y.F. Dufrêne, Nanoscale analysis of supported lipid bilayers using atomic force microscopy, Biochim. Biophys. Acta Biomembr. 1798 (2010) 750–765, https://doi.org/10.1016/j.bbamem.2009.07.026.
[57] P. Szekely, T. Dvir, R. Asor, R. Resh, A. Steiner, O. Szekely, A. Ginsburg, J. Mosenkis, V. Guralnick, Y. Dan, T. Wolf, C. Tamburu, U. Raviv, Effect of temperature on the structure of charged membranes, J. Phys. Chem. B 115 (2011) 14501–14506, https://doi.org/10.1021/jp207566n.
[58] A. Alessandrini, P. Facci, Phase transitions in supported lipid bilayers studied by AFM, Soft Matter 10 (2014) 7145–7164, https://doi.org/10.1039/C4SM01104J.
[59] L. Redondo-Morata, M.I. Giannotti, F. Sanz, Structural impact of cations on lipid bilayer models: Nanomechanical properties by AFM-force spectroscopy, Mol. Membr. Biol. 31 (2014) 17–28, https://doi.org/10.3109/09687688.2013.868940.
[60] B. Gumí-Audenis, L. Costa, F. Carlá, F. Comin, F. Sanz, M. Giannotti, Structure and nanomechanics of model membranes by atomic force microscopy and spectroscopy: insights into the role of cholesterol and sphingolipids, Membranes 6 (2016) 58, https://doi.org/10.3390/membranes6040058.
[61] A.V.R. Murthy, F. Guyomarc'h, C. Lopez, The temperature-dependent physical state of polar lipids and their miscibility impact the topography and mechanical properties of bilayer models of the milk fat globule membrane, Biochim. Biophys. Acta Biomembr. 1858 (2016) 2181–2190, https://doi.org/10.1016/j.bbamem.2016.06.020.
[62] S. Garcia-Manyes, L. Redondo-Morata, G. Oncins, F. Sanz, Nanomechanics of lipid bilayers: heads or tails? J. Am. Chem. Soc. 132 (2010) 12874–12886, https://doi.org/10.1021/ja1002185.
[63] A.V.R. Murthy, F. Guyomarc'h, C. Lopez, Palmitoyl ceramide promotes milk sphingomyelin gel phase domains formation and affects the mechanical properties of the fluid phase in milk-SM/DOPC supported membranes, Biochim. Biophys. Acta Biomembr. 1860 (2018) 635–644, https://doi.org/10.1016/j.bbamem.2017.12.005.
[64] V.I. Uricanu, M.H.G. Duits, J. Mellema, Hierarchical networks of casein proteins: an elasticity study based on atomic force microscopy, Langmuir 20 (2004) 5079–5090, https://doi.org/10.1021/la0363736.
[65] T. Hianik, Mechanical properties of lipid bilayers and protein-lipid interactions, in: F. Bersani (Ed.), Electr. Magn. Biol. Med, Springer US, Boston, MA, 1999, pp. 235–238, , https://doi.org/10.1007/978-1-4615-4867-6_52.
[66] H. Khandelia, J.H. Ipsen, O.G. Mouritsen, The impact of peptides on lipid membranes, Biochim. Biophys. Acta Biomembr. 1778 (2008) 1528–1536, https://doi.org/10.1016/j.bbamem.2008.02.009.
[67] G. Andre, R. Brasseur, Y.F. Dufrêne, Probing the interaction forces between hydrophobic peptides and supported lipid bilayers using AFM, J. Mol. Recognit. 20 (2007) 538–545, https://doi.org/10.1002/jmr.837.
[68] D.G. Cornell, R.J. Carroll, Miscibility in lipid-protein monolayers, J. Colloid Interface Sci. 108 (1985) 226–233, https://doi.org/10.1016/0021-9797(85)90254-1.
[69] F. Wang, S. Sui, Phase separation of phospholipid monolayers induced by membrane penetration of human apolipoprotein H, Colloids Surf. A Physicochem. Eng. Asp. 198–200 (2002) 281–286, https://doi.org/10.1016/S0927-7757(01)00943-8.
[70] I. Rødland, Ø. Halskau, A. Martínez, H. Holmsen, α-Lactalbumin binding and membrane integrity—effect of charge and degree of unsaturation of glycerophospholipids, Biochim. Biophys. Acta Biomembr. 1717 (2005) 11–20, https://doi.org/10.1016/j.bbamem.2005.09.004.
[71] D.V. Brooksbank, J. Leaver, D.G. Dalgleish, Adsorption of milk proteins to phosphatidylglycerol and phosphatidylcholine liposomes, J. Colloid Interface Sci. 161 (1993) 38–42.
[72] Y. Fang, D.G. Dalgleish, Structures and properties of vesicles formed from phospholipids and caseins, Food Res. Int. 29 (1996) 201–206, https://doi.org/10.1016/0963-9969(95)00066-6.
[73] J.B. Li, A study of mixed phospholipid/b-casein monolayers at the water|air surface, Colloids Surf. A Physicochem. Eng. Asp. 142 (1998) 355–360.
[74] A.L. Caro, M.R.R. Niño, J.M.R. Patino, The effect of pH on structural, topographical, and rheological characteristics of β-casein–DPPC mixed monolayers spread at the air–water interface, Colloids Surf. A Physicochem. Eng. Asp. 332 (2009) 180–191, https://doi.org/10.1016/j.colsurfa.2008.09.020.
[75] A. Herrig, M. Janke, J. Austermann, V. Gerke, A. Janshoff, C. Steinem, Cooperative adsorption of Ezrin on PIP2-containing membranes, Biochemistry (Mosc) 45 (2006) 13025–13034, https://doi.org/10.1021/bi061064a.
[76] R.P. Richter, J. Lai Kee Him, B. Tessier, C. Tessier, A.R. Brisson, On the kinetics of adsorption and two-dimensional self-assembly of Annexin A5 on supported lipid bilayers, Biophys. J. 89 (2005) 3372–3385, https://doi.org/10.1529/biophysj.105.064337.
[77] A.P. Minton, Effects of excluded surface area and adsorbate clustering on surface adsorption of proteins. II. Kinetic models, Biophys. J. 80 (2001) 1641–1648, https://doi.org/10.1016/S0006-3495(01)76136-X.
[78] M. Rabe, D. Verdes, S. Seeger, Understanding cooperative protein adsorption events at the microscopic scale: a comparison between experimental data and Monte Carlo simulations, J. Phys. Chem. B 114 (2010) 5862–5869, https://doi.org/10.1021/jp909601m.
[79] A. Hinderliter, S. May, Cooperative adsorption of proteins onto lipid membranes, J. Phys. Condens. Matter 18 (2006) S1257–S1270, https://doi.org/10.1088/0953-8984/18/28/S09.
[80] G.W. Feigenson, Calcium ion binding between lipid bilayers: the four-component system of phosphatidylserine, phosphatidylcholine, calcium chloride, and water, Biochemistry (Mosc) 28 (1989) 1270–1278, https://doi.org/10.1021/bi00429a048.
[81] J. Huang, J.E. Swanson, A.R. Dibble, A.K. Hinderliter, G.W. Feigenson, Nonideal mixing of phosphatidylserine and phosphatidylcholine in the fluid lamellar phase, Biophys. J. 64 (1993) 413–425, https://doi.org/10.1016/S0006-3495(93)81382-1.
[82] T.N. Murugova, P. Balgavý, Molecular volumes of DOPC and DOPS in mixed bilayers of multilamellar vesicles, Phys. Chem. Chem. Phys. 16 (2014) 18211–18216, https://doi.org/10.1039/C4CP01980F.
[83] V.H. Teixeira, D. Vila-Viçosa, P.B.P.S. Reis, M. Machuqueiro, Values of titrable amino acids at the water/membrane interface, J. Chem. Theory Comput. 12 (2016) 930–934, https://doi.org/10.1021/acs.jctc.5b01114.
[84] A.L. Caro, M.R. Rodríguez Niño, J.M. Rodríguez Patino, Dynamics of penetration of dipalmitoyl-phosphatidyl-choline (DPPC) monolayers by β-casein, Colloids Surf. A Physicochem. Eng. Asp. 341 (2009) 134–141, https://doi.org/10.1016/j.colsurfa.2009.03.056.
[85] G. van Meer, Lipids of the Golgi membrane, Trends Cell Biol. 8 (1998) 29–33, https://doi.org/10.1016/S0962-8924(97)01196-3.
[86] G. van Meer, D.R. Voelker, G.W. Feigenson, Membrane lipids: where they are and how they behave, Nat. Rev. Mol. Cell Biol. 9 (2008) 112–124, https://doi.org/10.1038/nrm2330.
[87] P.J. Quinn, Plasma membrane phospholipid asymmetry, Subcell. Biochem. 36 (2002) 39–60.
[88] C. Lopez, Milk fat globules enveloped by their biological membrane: unique colloidal assemblies with a specific composition and structure, Curr. Opin. Colloid Interface Sci. 16 (2011) 391–404, https://doi.org/10.1016/j.cocis.2011.05.007.
[89] C. Lopez, C. Cauty, F. Guyomarc'h, Organization of lipids in milks, infant milk formulas and various dairy products: role of technological processes and potential impacts, Dairy Sci. Technol. 95 (2015) 863–893, https://doi.org/10.1007/s13594-015-0263-0.